Breast Cancer: Targets and Therapy

Dovepress
open access to scientific and medical research

Open Access Full Text Article

ORIGINAL RESEARCH

A Comprehensive Model Based on Dynamic Contrast-Enhanced Magnetic Resonance Imaging Can Better Predict the Preoperative Histological Grade of Breast Cancer Than a Radiomics Model

Yitian Wu[1], Weixing Pan[2], Lingxia Wang[3], Wenting Pan[2], Huangqi Zhang[2], Shengze Jin[1], Xiuli Wu[4], Aie Liu[5], Enhui Xin[5], Wenbin Ji[6,7]

[1]School of Medicine, Shaoxing University, Shaoxing, Zhejiang, 312000, People's Republic of China; [2]Department of Radiology, Taizhou Hospital of Zhejiang Province Affiliated to Wenzhou Medical University, Linhai, Zhejiang, 317000, People's Republic of China; [3]Department of Radiology, Taizhou Hospital, Zhejiang University, Taizhou, Zhejiang, 317000, People's Republic of China; [4]Department of Nuclear Medicine, Taizhou Hospital of Zhejiang Province, Linhai, Zhejiang, 317000, People's Republic of China; [5]Department of Research Center, Shanghai United Imaging Intelligence Co., Ltd, Shanghai, 200000, People's Republic of China; [6]Department of Radiology, Taizhou Hospital of Zhejiang Province, Shaoxing University, Taizhou, Zhejiang, 312000, People's Republic of China; [7]Key Laboratory of Evidence-Based Radiology of Taizhou, Linhai, Zhejiang, 317000, People's Republic of China

Correspondence: Wenbin Ji, Email wb.j@163.com

Background: Histological grade is an important prognostic factor for patients with breast cancer and can affect clinical decision-making. From a clinical perspective, developing an efficient and non-invasive method for evaluating histological grading is desirable, facilitating improved clinical decision-making by physicians. This study aimed to develop an integrated model based on radiomics and clinical imaging features for preoperative prediction of histological grade invasive breast cancer.

Methods: In this retrospective study, we recruited 211 patients with invasive breast cancer and randomly assigned them to either a training group (n=147) or a validation group (n=64) with a 7:3 ratio. Patients were classified as having low-grade tumors, which included grade I and II tumors, or high-grade tumors, which included grade III tumors. Three models were constructed based on basic clinical features, radiomics features, and the sum of the two. To assess diagnostic performance of the radiomics models, we employed measures such as receiver operating characteristic (ROC) curve, decision curve analysis (DCA), accuracy, sensitivity, and specificity, and the predictive performance of the three models was compared using the DeLong test and net reclassification improvement (NRI).

Results: The area under the curve (AUC) of the clinical model, radiomics model, and comprehensive model was 0.682, 0.833, and 0.882 in the training set and 0.741, 0.751, and 0.836 in the validation set, respectively. NRI analysis confirmed that the combined model was better than the other two models in predicting the histological grade of breast cancer (NRI=21.4% in the testing cohort).

Conclusion: Compared with the other models, the comprehensive model based on the combination of basic clinical features and radiomics features exhibits more significant potential for predicting histological grade and can better assist clinicians in optimal decision-making.

Keywords: breast cancer, histological grade, magnetic resonance imaging, radiomics, comprehensive model, NRI

Introduction

According to the GLOBOCAN 2018 data produced by the International Agency for Research on Cancer from 185 countries, 2.3 million new breast cancer cases were reported, with a mortality rate of 6.9%.[1] Breast cancer has become the most common cancer globally and is responsible for the high proportion of cancer-related deaths among women; therefore, prognosis is crucial in the diagnosis and treatment of breast cancer. Tumor histopathological grade,[2–4] positive estrogen and progesterone receptors,[5] and lymph node metastasis[6] are important independent prognostic factors for patients with breast cancer and play essential roles in clinical treatment. Therefore, determining the histological grade of the tumor using breast cancer imaging can provide a significant breakthrough.

Received: 13 July 2023
Accepted: 30 September 2023
Published: 18 October 2023

Clinically, the most common method for histological grading involves examining breast tissue sections after surgery or core biopsy. However, obtaining the histological grade through surgery or core biopsy is both time-consuming and costly, and it cannot be accomplished prior to the surgical procedure. Therefore, it is necessary to find a preoperative, non-invasive, and effective method to predict the histological grade of breast cancer.

With further developments in imaging technology, breast magnetic resonance imaging (MRI) plays an essential role in the diagnosis of breast cancer. Radiomics based on breast magnetic resonance is a new technique for predicting neoadjuvant chemotherapy response,[7] Ki-67 expression level,[8–10] benign or malignant tumor,[11] and breast cancer recurrence[12] and plays an essential role in the clinical diagnosis and detection of breast cancer. It converts standard magnetic resonance images into specific radiological features and then selects the most relevant features as an essential basis for diagnosing tumors or diseases. However, only few studies are available on integrated models combining clinical and MRI features and radiomics to predict the histological grade of breast cancer. Wang et al[13] reported a histological grading model for predicting performance, but the efficacy was not satisfactory.

Therefore, we aimed to develop a comprehensive model based on dynamic contrast-enhanced MRI (DCE-MRI) to predict the histological grade of breast cancer. The feasibility and accuracy of the comprehensive model of clinical and MRI features in the preoperative evaluation of breast cancer have been discussed, as the model may serve as a foundation for early accurate diagnosis and a reasonable treatment plan.

Materials and Methods

Study Population

This retrospective study included 211 patients (219 lesions) who were surgically diagnosed with invasive breast cancer from January 2016 to July 2022. The inclusion criteria were as follows: (a) routine MRI and DCE-MRI within 2 weeks before surgery, (2) no surgery, radiotherapy, or chemotherapy before examination, and (c) complete clinicopathological data and medical images. The exclusion criteria were as follows: (a) poor image quality, (b) incomplete clinical data, and (C) diffuse lesions that could not be delineated with region of interest (ROI).

We randomly divided patients into the training (n=147) and validation cohorts (n=64) in a ratio of 7:3. A study flow diagram is presented in Figure 1. Because grade III tumors exhibit more aggressive molecular biology features reflecting worse prognosis,[14] we defined histological grade I and II tumors as the low-grade group and histological grade III tumors as the high-grade group.

This retrospective study was approved by the Institutional Review Board of Taizhou Hospital of Zhejiang Province, Affiliated to Wenzhou Medical University, and the requirement for obtaining written informed consent was waived. Informed consent was waived by our Institutional Review Board because of the retrospective nature of our study. The personal information of patients was strictly protected. The authors confirmed that the ethical principle was followed in the Declaration of Helsinki.

MRI Techniques

The examinations were performed using 1.5 T MR (Signa HDxt 1.5 T, GE Healthcare, USA) or 3.0 T MR (Discover MR 750 3.0 T, GE Healthcare, USA) with a special phased-array surface coil for the breast. The patients were placed in the prone position with the unilateral breast naturally suspended in the breast coils for scanning. Axial lava sequence scanning was performed to obtain DCE-MRIs. The contrast agent used was gadopentetate dimeglumine (Guangzhou Kangshen Pharmaceutical Co., Ltd.). The dose of intravenous bolus injection was 0.1 mmol/kg, and the rate was 2.5 mL/s. After the contrast agent was injected, 20 mL of normal saline was injected at the same rate. The mask was acquired before enhancement. Scanning was performed seven consecutive times, 15s after the contrast agent was injected. DCE-MRI consists of eight stages, with a single scanning time of 51s. The first four stages were separated by 1 s, and the 5th, 6th, and 7th stages were separated by 60s, with a total time of 9 min. The scanning parameters were as follows: TR, 3.9 ms; TE, 2.2 ms; flip angle (FA), 5°; FOV, 360 mm × 360 mm; matrix, 320×320 mm; no interval scanning. For 1.5 T MR, eight images were obtained, with a scanning time of 63s for each image post-contrast. The scanning parameters were as follows: TR, 6.1 ms; TE, 3.0 ms; flip angle (FA), 1.5°; FOV, 330×330 mm.

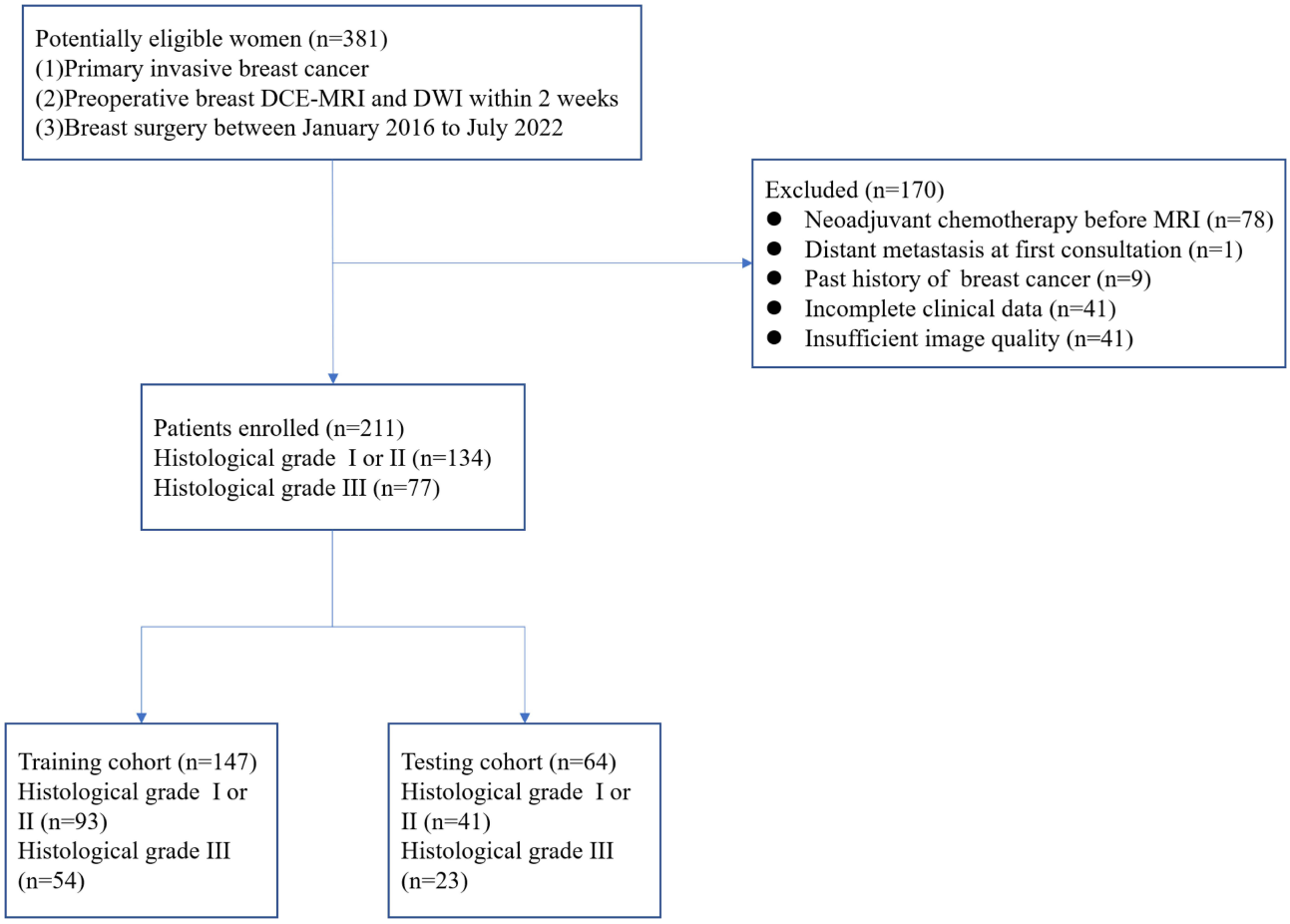

Figure 1 Flowchart of the study population.

MRI Image Analysis

To assess tumor morphology, all MR images were reviewed independently by two breast radiologists (one with 1 year and one with 3 years of experience), regardless of patient clinical history. Tumor location, diameter, lymph nodes, margin, edge enhancement pattern, morphology and Apparent diffusion coefficient (ADC) signal were evaluated. Axillary lymph node enlargement was defined as one or more of the following manifestations: abnormal lymph node morphology, increased cortical thickness, irregular lymph node margins, or complete or partial disappearance of the fatty hilum.

Radiomics Analysis

Workflow

Radiomics analysis was performed using the uAI Research Portal (Shanghai United Imaging Intelligent Medical Technology Co., Ltd.) embedded into the widely used package PyRadiomics (https://pyradiomics.readthedocs.io/en/latest/index.html)[15] The radiomics workflow comprised tumor segmentation, feature extraction, feature selection, and model construction and evaluation (Figure 2).

Image Processing and Segmentation

In this study, the ROI was sketched based on the second phase of DCE-MRI (67 s after the injection of contrast medium). We used a 3D RU-net for automatic tumor segmentation. This tool has been used in a multicenter test data set, and the dice coefficient of the validation set was >0.75 in 422 participants.[16]

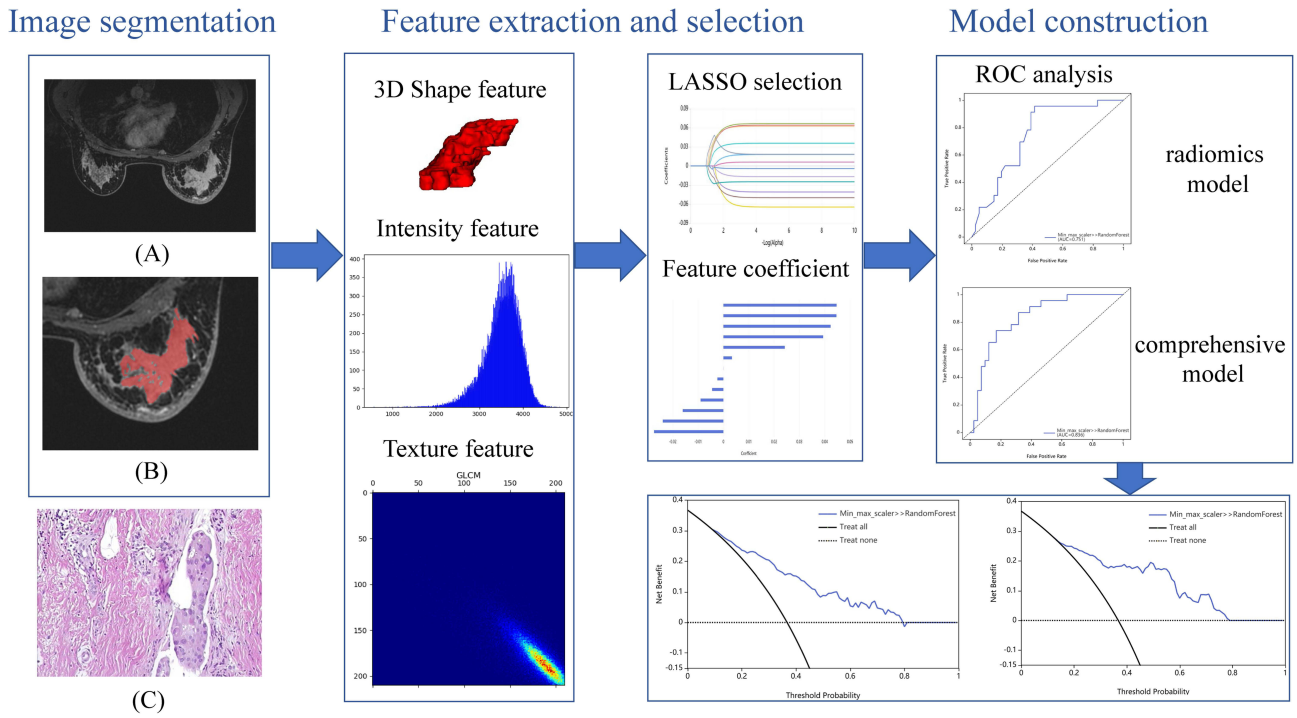

Figure 2 Workflow of Radiomics Analysis. (**A**) Second phase of DCE-MRI with no ROI drawn (**B**) Delineated ROI (**C**) Pathological section of the patient.

Subsequently, a radiologist with 3 years of experience adjusted the tumor range according to the DWI and DCE-MRI. When there were multiple tumors, the largest tumor was selected as the target tumor.

Feature Extraction

The images were imported into the uAI Research Portal (Shanghai United Imaging Intelligent Medical Technology Co., Ltd.) and 104 radiomics features were extracted within the lesion annotation range from DCE-MRI. These radiomics features included First Order Statistics, Shape, Gray Level Cooccurrence Matrix, Gray Level Size Zone Matrix, Gray Level Run Length Matrix, Neighboring Gray Tone Difference Matrix, and Gray Level Dependence Matrix features. Twenty-five imaging filters (eg, Wavelet and Gaussian) provided by the uAI Research Portal were used for feature extraction. Consequently, 2264 features were obtained.

Feature Selection

To avoid over-fitting the imaging features, the features were further selected in two steps before constructing the imaging features. First, the feature of *t*-test P <0.05 in the training queue was retained. After Z-score normalization, each feature was selected by least absolute shrinkage and selection operator regression (LASSO). According to Harrell's guideline, the number of selected features should be <10% of the sample size. Therefore, the number of features used for subsequent model construction was determined to be less than 20.

Model Construction and Evaluation

To maximize the discrimination of the radiomics algorithm, a random forest machine learning classifier was implemented for model construction.

For model evaluation, the receiver operating characteristic curves (ROC) were plotted, and the area under the curve (AUC), decision curve analysis (DCA), accuracy, sensitivity, and specificity were calculated to quantify the predictive efficacy. Subsequently, a calibration curve was plotted to estimate the coincidence between the prediction model and actual outcomes. Finally, the net reclassification improvement (NRI) and DeLong tests were used to assess the clinical usefulness of the prediction model.

Statistical Analysis

MedCalc (edition 20.0; MedCalc statistical software-free trial available) and R software (version 4.1.1, http://www.r-project.org) were used for statistical analysis. The Kolmogorov–Smirnov test was used to test whether the measurement data fit the Gaussian distribution. Data consistent with a normal distribution were represented as x±s, and Student's *t*-test was conducted. Non-normally distributed data are presented as median (interquartile interval) and examined using the Mann–Whitney *U*-test. Categorical variables are expressed as number of cases (percentage), and chi-square or Fisher's exact tests were performed. We compared the models using the NRI and DeLong test to select the best model. Statistical significance was set at $P < 0.05$, and multivariate Cox regression analysis was performed to determine significant variables.

Pathological and Immunohistochemical Examination

The histological grade of patients with invasive breast cancer was assessed using the Nottingham Modified Scarff–Bloom–Richardson (SBR) grading system, which includes the following: (1) the proportion of glandular ducts formed, (2) nuclear pleomorphism, and (3) mitotic image counting. Each index was evaluated separately and given a score of 1–3, and the scores of the three indices were combined. A score of 3–5 was classified as histological grade I, 6–7 as grade II, and 8–9 as grade III.[17]

Immunohistochemical results were evaluated according to the American Society of Clinical Oncology/College of American Pathologists Guideline 2019. Estrogen receptor (ER) or progesterone receptor (PR) was considered positive if 1–100% of the tumor cell nuclei in the samples showed an immune response to the test.[18] Tumors with Ki-67 expression lower than 14% were considered negative, while the others were considered positive.[19]

Results

Clinicopathological Factors

Overall, 211 patients were enrolled in this study, including 26 with grade I tumors, 108 with grade II tumors, and 77 with grade III tumors.

The clinicopathological features presented in Table 1 indicate that histologic grade III lesions had a pathological diameter between 2 and 5 cm more frequently than histologic grades I and II lesions (51.9% [41/77] vs 35.1% [47/134], $P = 0.04$). Moreover, regarding palpate size, a greater proportion of grade III lesions were between 2 and 5 cm in diameter than low-grade lesions (53% [38/77] vs 11.2% [16/134], $P = 0.04$). Grade III histological lesions were more likely to be ER-negative (47.5% [38/77] vs 11.2% [16/134], $P < 0.01$) and PR-negative (61.0% [47/77] vs 17.9% [24/134], $P < 0.01$) than the other groups. The positive expression of Ki-67 in the grade III group was higher than that in the other groups (100% [77/77] vs 68.7% [92/134], $P < 0.01$). There were no statistically significant differences in age, body mass index, menses-related variables, palpation texture, lymph node metastasis and magnetic field strength between the two groups ($P > 0.05$).

MRI Features

Table 2 summarizes the basic features of the lesions on MRI and analyzes the relationship between these features and histological grade. Histologic grades I and II tumors were smaller than 2 cm (65.3% [64 of 59] vs 44.1% [26 of 98], $P < 0.01$). However, grade III tumors were mainly between 2 and 5 cm in size (54.2% [32 of 59] vs 32.7% [32 of 98], $P = 0.02$). Histological grade was significantly associated with margin and boundary ($P < 0.05$) (Table 2). There was no significant difference in tumor location, lymph node status, lesion shape, and enhancement between the two groups ($P > 0.05$). The ICC or Kappa test between observers indicated good consistency (Table 2).

Construction of Clinical, Radiomics, and Comprehensive Models

Three paradigms of tumor segmentation results are presented in Figure 3. Overall, 2264 radiomics features were extracted from the MR images. Using the *t*-test, 320 features were observed to have a significant effect in discriminating histological grades. These features were then z-score normalized, and LASSO was used to obtain the most valuable features, resulting in 13 key features and a radiomic-score. The first four most representative of these characteristics are: Informational Measure of Correlation 1, which assesses the correlation between the probability distributions (quantifying

Table 1 Patient Demographics in 211 Women and Characteristics of 219 Breast Lesions

Parameter	I+II(n=134)	III(n=77)	t /F /χ2 value	P value
Age(y)†, median(IQR)	50.0(48.0–51.0)	51.0(47.4–54.6)	−1.620	0.11
BMI(kg/m2)†, median(IQR)	23.5(23.1–24.1)	23.3(22.4–23.9)	−0.490	0.62
Menstruation				
Age of Menarche(y)†, median(IQR),	14.0(14.0–14.0)	14.0(14.0–14.6)	0.005	1.00
Duration of menstruation(d)†, median(IQR)	5.0(4.5–5.0)	5.0(4.5–5.5)	−0.550	0.58
Menstrual cycle(d)†, median(IQR)	29.0(29.0–29.0)	29.0(29.0–29.0)	−0.470	0.64
Age of marriage(y)†, median(IQR)	25.0(24.7–25.0)	24.0(23.0–25.0)	1.510	0.13
Palpation texture, n(%)			0.247	0.88
Soft	30(22.4)	15(19.5)		
Hard	25(18.6)	15(19.5)		
Harder	79(59.0)	47(61.0)		
Palpation Diameter(cm), n(%)			18.14	0.01*
<2	79(59.0)	23(30.0)		
2~5	52(38.8)	53(68.8)		
≥5	3(2.2)	1(1.2)		
Pathological diameter(cm), n(%)			6.288	0.04*
<2	83(61.9)	34(44.2)		
2~5	47(35.1)	40(51.9)		
≥5	4(3.0)	3(3.9)		
Lymph node, n(%)			0.996	0.07
No Metastasis	67(50.0)	44(57.1)		
Metastasis	67(50.0)	33(42.9)		
ER, n(%)			35.769	0.01*
Negative	16(11.2)	38(47.5)		
Positive	118(88.8)	39(52.5)		
PR, n(%)			40.547	0.01*
Negative	24(17.9)	47(61.0)		
Positive	110(82.1)	30(39.0)		
Ki-67, n(%)			/	0.01*
Negative	42(31.3)	0(0.0)		
Positive	92(68.7)	77(100.0)		
Magnetic field strength, n(%)			0.077	0.78
1.5T	74(55.2)	41(53.2)		
3.0T	60(44.8)	36(46.8)		

Notes: Data are number of women or number of lesions, and data in parentheses are percentages. †Data are median; data in parentheses are interquartile range. The table is divided into two parts; the bottom half contains pathological information, which we did not use for modeling. *P < 0.05.

Abbreviations: IQR, interquartile range; BMI, Body Mass Index; ER, Estrogen Receptor; PR, Progesterone Receptor.

the complexity of the texture); Large Area Low Gray Level Emphasis, which measures the proportion in the image of the joint distribution of larger size zones with lower gray-level values; Large Dependence High Gray Level Emphasis, which measures the joint distribution of large dependence with higher gray-level values; and Skewness, which measures the asymmetry of the distribution of values about the Mean value. Finally, a radiomics model was established using 14 features. The clinical and MRI features that were statistically significant in the univariate analysis were subjected to multiple logistic regression (Table 3), and finally, two features (palpate size and margin) were considered statistically significant. These two features were used to build a clinical model, and the two features and 14 key features were used to build a comprehensive model.

Table 4 summarizes the discrimination performance of each model. The clinical model had good performance in the AUC, sensitivity, specificity and accuracy of distinguishing histological grade in the training cohort and test cohort. In contrast, radiomics was superior to the clinical model in identifying histological grades, with an AUC of 0.751 (0.630–

Table 2 Lesion Characteristics at DCE-MRI

Parameter	I+II(n=134)	III(n=77)	Kappa / ICC	t /F /χ2 value	P value
Situs, n(%)			/	0.629	0.43
Left	72(53.7)	37(48.1)			
Right	62(46.3)	40(51.9)			
MRI Diameter(cm), n(%)			0.886	7.41	0.02*
<2	85(63.4)	34(44.2)			
2~5	47(35.1)	41(53.2)			
≥5	2(1.5)	2(2.6)			
Lymph node, n(%)			0.848	4.393	0.11
Enlargement	7(5.2)	7(9.1)			
Display	66(49.3)	27(35.1)			
Normal	61(45.5)	43(55.8)			
Boundary, n(%)			0.765	4.123	0.04*
Clarity	47(35.1)	38(49.4)			
Blur	87(64.9)	39(50.6)			
Margin, n(%)			0.747	6.428	0.04*
Smooth	20(15.0)	20(26.0)			
Spicule	57(42.5)	36(46.8)			
Lobular	57(42.5)	21(27.2)			
Morphology, n(%)			0.875	0.618	0.73
Cycle	15(11.2)	10(13.0)			
Oval	30(22.4)	20(26.0)			
Irregular	89(66.4)	47(61.0)			
Enhancement pattern, n(%)			0.774	3.003	0.22
Homogeneous	34(25.4)	14(18.2)			
Heterogeneous	88(65.7)	51(66.2)			
Annular	12(8.9)	12(15.6)			
ADC values on DWI(× 10–3 mm /s)†, median(IQR)	916(865–940)	(884–956)	0.746	−1.376	0.17

Notes: Data are number of women or number of lesions, and data in parentheses are percentages. †Data are median; data in parentheses are interquartile range. *P < 0.05.

Abbreviations: IQR, interquartile range; ADC= apparent diffusion coefficient; DWI, diffusion weighted imaging.

0.871) in the test cohort. Finally, our developed integrated model achieved better results in distinguishing histological grades (Figure 4). The AUC of 0.836 (0.736–0.935), sensitivity, specificity, and accuracy of both the training and test sets were better than those of the other two models.

By calculating the NRI of the continuous variables in the training set, the comprehensive model was better than the radiomics model, and the radiomics model was better than the clinical model (Table 5). The DeLong test statistical p-value of the comprehensive and the radiation models was 0.067, and the p-value of the comprehensive and the clinical models was 0.194.

Discussion

In this study, we established and compared three classification models to predict the histological grade of patients with breast cancer before surgery. The results showed that our comprehensive model was significantly better than the other two models in predicting the preoperative histological grade of patients with breast cancer.

In this study, histological grades I and II were classified as one group and histological grade III as a separate group. According to a long-term follow-up study of 2219 patients, histological grade was critical for determining the prognosis of patients with breast cancer. When comparing the individual grade categories, the least difference was observed between histological grades I and II.[20]

Many previous studies have shown that histological grading is a definite prognostic factor for breast cancer.[2,3] It represents a morphological assessment of the biological characteristics of breast cancer and has been shown to provide information

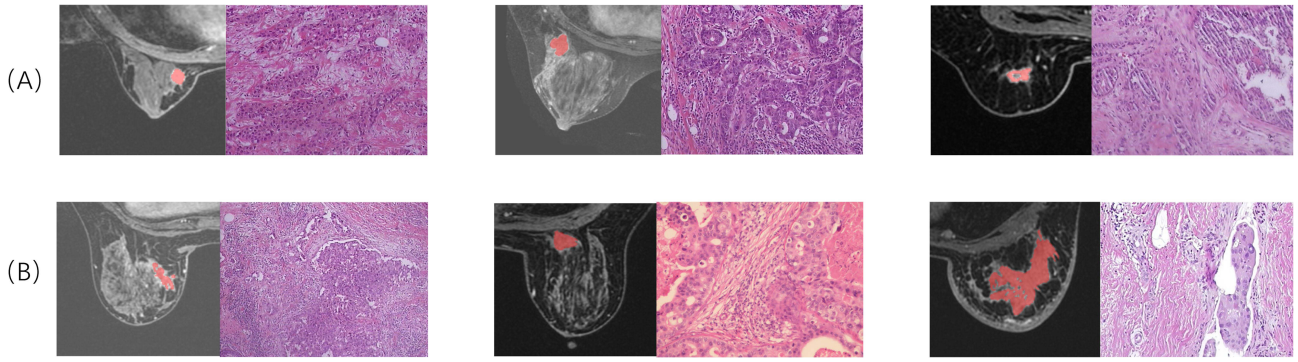

Figure 3 Six paradigms of tumor segmentation results. (**A**) Three patients had a low histopathological grade. (**B**) Three patients with high histopathological grades.

related to its clinical behavior.[4] Determining the histological grades can be challenging task, often necessitating preoperative invasive biopsies or the examination of surgically resected tissue samples for pathological microscopic evaluation.

Value of Clinical and MRI Parameters on DCE-MRI

In this study, we measured the maximum tumor diameter on MRI and converted the numerical variable into a categorical variable based on the TNM staging of breast cancer. The results showed that the diameter measured on MRI, palpation, and pathology in patients with histological grade III was mostly in the range of 2–5 cm, whereas lesions smaller than 2 cm were mostly found in patients with histological grades I and II. This is consistent with the results of previous studies which showed that the proportion of histological grade III tumors was higher in larger tumors.[21] Heusinger et al demonstrated that palpation can effectively assess tumor size before surgery.[22] This corresponds with our findings. In addition, we found that the margin and boundary were statistically significant for histological grading. Alduk et al showed that high-grade breast cancer often presents with smooth margins, whereas low-grade breast cancer presents with needle-like margins, and margins are adverse prognostic factors.[23] Our study showed that high-grade tumors had smooth margins relative to low-grade tumors. In addition, our study showed that ADC values were not associated with histological grade, which may be related to our low sample size. Previous studies have reported that ADC value is negatively correlated with histological grade, and low ADC value predicts more advanced histological grade.[24,25]

Table 3 Multivariate Logistic Regression Analysis of Features Associated with Histological Grade

Variable	Odds Ratio	95% CI	P value
Palpation Diameter			
<2			
2~5	3.2853	1.6738–6.4485	0.0005*
≥5	0.7112	0.0400–12.6361	0.8165
MRI Diameter			
<2			
2~5	1.6325	0.8422–3.1644	0.1467
≥5	3.6442	0.2769–47.9545	0.3254
Boundary	0.6306	0.3132–1.2698	0.1967
Margin			
Smooth			
Spicule	0.5437	0.2354–1.2561	0.1538
Lobular	0.3771	0.1448–0.9817	0.0457*

Notes: *P < 0.05.

Table 4 Performance of Three Model in the Training and Testing Cohorts

Model	Training Cohort (n=147)				Testing Cohort (n=64)			
	AUC (95% CI)	SEN	SPE	ACC	AUC (95% CI)	SEN	SPE	ACC
Clinical Model	0.682(0.596–0.767)	0.574	0.677	0.639	0.741(0.619–0.863)	0.652	0.634	0.641
Radiomics Model	0.833(0.769–0.896)	0.778	0.688	0.721	0.751(0.630–0.871)	0.696	0.659	0.672
Comprehensive Model	0.882(0.828–0.936)	0.852	0.806	0.823	0.836(0.736–0.935)	0.739	0.829	0.797

Abbreviations: AUC, area under the curve; SEN, sensitivity; SPE, specificity; ACC, accuracy; 95% CI, 95% confidence interval.

However, another multicenter analysis showed that ADC could not be used as a surrogate marker for Ki-67 and histological grade.[26]

Comparison Between Models

Radiomics is widely used in various medical fields, including pancreatic tumors, prostate cancer, and breast cancer lymphatic metastasis.[27–29] In 2021, He et al[28] used an MRI-based radiomics model to show good performance in distinguishing benign and malignant prostate lesions. Yu et al[29] developed clinical-radiomic nomograms that were useful in clinical decision-making associated with personalized selection of surgical interventions and therapeutic regimens for patients with early-stage breast cancer. Liu et al[27] used radiomics to distinguish benign and malignant breast cancer, and the effect was better than the Breast Imaging-Reporting and Data System classification. Before this study, Wang et al[13] reported a good histological grading predictive performance model for 901 patients, with an AUC value of 0.722. In this

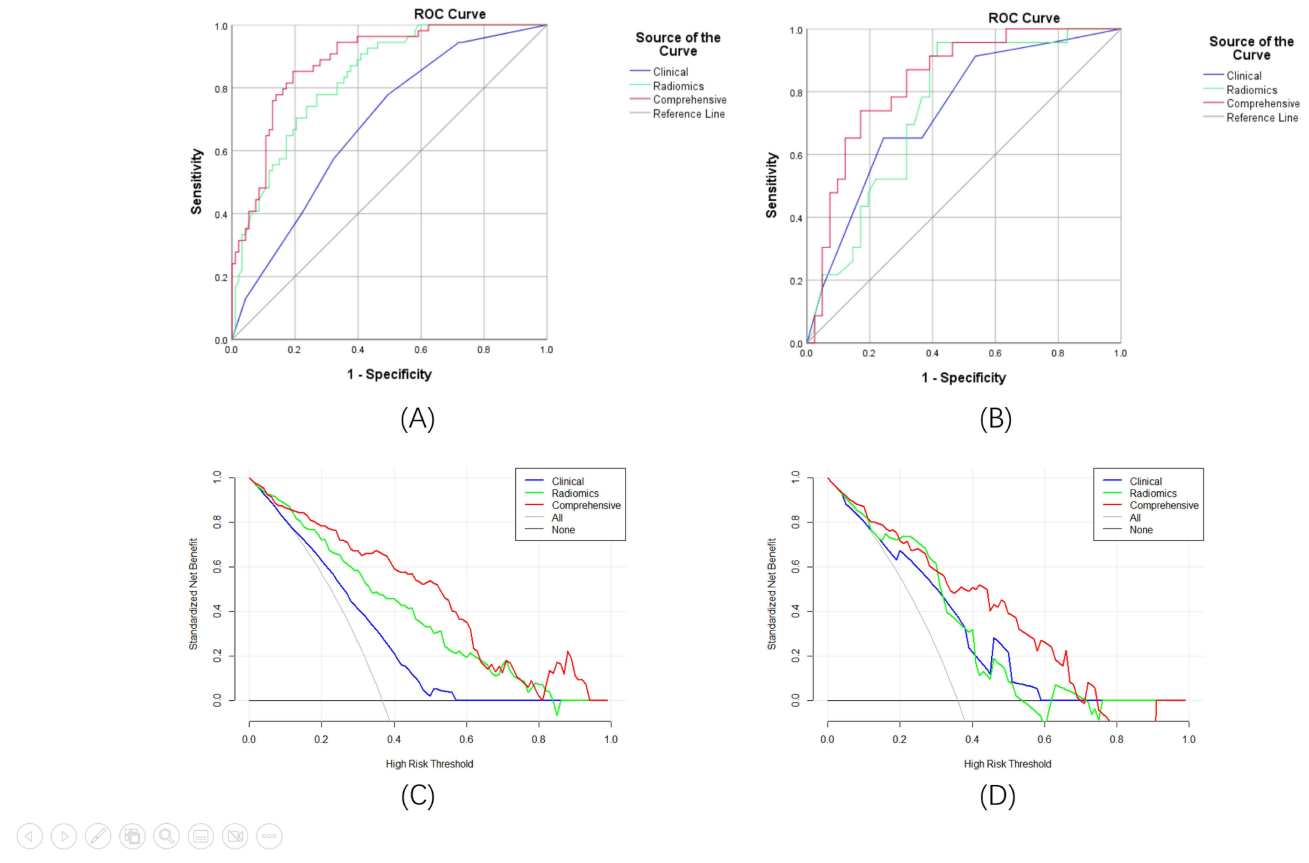

Figure 4 Receiver operator characteristic (ROC) curves, calibration curve, and decision curve analysis (DCA) of three models. (**A**) Three models of ROC curves in the training cohort. (**B**) Three models of ROC curves in the testing cohort. (**C**) Three models of decision curve analysis (DCA) curve in the training cohort. (**D**) Three models of decision curve analysis (DCA) in the testing cohort.

Table 5 NRI of Three Model in the Training and Testing Cohorts

Model	Training Cohort		Testing Cohort	
	NRI	P(NRI)	NRI	P(NRI)
Comprehensive vs Radiomics	19.20%	0.003	21.40%	0.039
Radiomics vs Clinical	21.40%	0.025	6.80%	0.328
Comprehensive vs Clinical	40.70%	<0.01	28.20%	0.025

Abbreviation: NRI, net reclassification improvement.

study, we first used 3DRU-net for automatic tumor segmentation and then manually checked and adjusted part of the ROI, which can better reflect the integrity of the tumor than 2D segmentation. The results showed that the radiomics model achieved an AUC of 0.833 in the training set and 0.751 in the validation set, which was not significantly different from the results of a previous study by Wang et al. Both the palpation size and margin were included in the comprehensive model (Table 4). We modeled statistically significant features for comparison, and the results were not unexpected—an AUC of 0.741 in the validation set was observed. However, when these two features (palpation size and margin) were fused, the AUC of the validation set of the comprehensive model reached 0.836, which was higher than the AUC of previous two models in terms of sensitivity, specificity, and accuracy. Therefore, the clinical information and radiomics features are complementary and can be combined to obtain features related to the histological grade of breast cancer.

The NRI showed that the comprehensive model was superior to the radiological and clinical models in terms of diagnostic performance, although the DeLong test p-value was 0.067. Thus, we can use the comprehensive model for preoperative prediction, and its performance is better than the other models.

The radiomics model misclassified 14 low-grade and 7 high-grade cancers in our validation cohort. In contrast, the comprehensive model misclassified seven low-grade cancers (five of which were the same as the radiomics model) and six high-grade cancers (four of which were the same as the radiomics model). These results show that the comprehensive model is superior to the radiomics model in identifying low-grade breast cancer, which can effectively prevent most of the upgrading of low-grade breast cancer and reduce the possibility of patients undergoing unnecessary treatment.

Limitations of This Study

Our study has the following limitations. First, because of the study's review nature, the loss of clinical information and MRI sequence in some patients resulted in a reduction in sample size. Second, the sample size of histological grade I tumors in this study was relatively small, which might have affected the efficacy of the statistical tests. However, in this study, grade I and II tumors were combined into one group, and the difference between this group and histological grade III was studied to minimize the impact of the sample size. Third, this is a retrospective study, not a prospective one, with the possibility of selection bias. Prospective studies are needed in the future to verify the results. Fourth, our study is a single-center study and did not use independent dataset pairs for external validation. Therefore, our study may not fully represent the general population and must be further verified in multicenter studies.

Conclusion

This study highlights the significant potential of the comprehensive model, which combines clinical and radiomics features, for predicting the histological grade of breast cancer. This comprehensive model can be regarded as a valuable non-invasive tool for histological grade prediction in breast cancer cases. We suggest that when patients are diagnosed with breast cancer before surgery, a comprehensive breast DCE-MRI should be performed to evaluate histological grading to make better clinical decisions.

Informed Consent Statement

The study was approved by the local ethics committee and informed consent was waived.

Acknowledgments

We would like to thank Editage for English language editing.

Funding

This study has received funding from the Zhejiang Provincial Medical and Health Science and Technology Program "Feasibility study of predicting recurrence and metastasis of triple-negative breast cancer based on radiomics model" (grant number: 2020KY359).

Disclosure

The authors declare no conflicts of interest related to this work.

References

1. Bray F, Ferlay J, Soerjomataram I, Siegel RL, Torre LA, Jemal A. Global cancer statistics 2018: GLOBOCAN estimates of incidence and mortality worldwide for 36 cancers in 185 countries. *CA Cancer J Clin*. 2018;68(6):394–424. doi:10.3322/caac.21492
2. Oshiro C, Yamasaki M, Noda Y, Nishimae A, Takahashi H, Inaji H. Comparative evaluation of nuclear and histological grades as prognostic factors for invasive breast cancer. *Breast Cancer*. 2020;27(5):947–953. doi:10.1007/s12282-020-01093-0
3. Escott CE, Zaenger D, Switchencko JM, et al. The influence of histologic grade on outcomes of elderly women with early stage breast cancer treated with breast conserving surgery with or without radiotherapy. *Clin Breast Cancer*. 2020;20(6):e701–e710. doi:10.1016/j.clbc.2020.05.007
4. Rakha EA, Reis-Filho JS, Baehner F, et al. Breast cancer prognostic classification in the molecular era: the role of histological grade. *Breast Cancer Res*. 2010;12(4):207. doi:10.1186/bcr2607
5. Yip CH, Rhodes A. Estrogen and progesterone receptors in breast cancer. *Future Oncol*. 2014;10(14):2293–2301. doi:10.2217/fon.14.110
6. Andersson Y, Frisell J, Sylvan M, de Boniface J, Bergkvist L. Breast cancer survival in relation to the metastatic tumor burden in axillary lymph nodes. *J Clin Oncol*. 2010;28(17):2868–2873. doi:10.1200/JCO.2009.24.5001
7. Braman NM, Etesami M, Prasanna P, et al. Intratumoral and peritumoral radiomics for the pretreatment prediction of pathological complete response to neoadjuvant chemotherapy based on breast DCE-MRI. *Breast Cancer Res*. 2017;19(1):57. doi:10.1186/s13058-017-0846-1
8. Huang Y, Wei L, Hu Y, et al. Multi-parametric MRI-based radiomics models for predicting molecular subtype and androgen receptor expression in breast cancer. *Front Oncol*. 2021;11:706733. doi:10.3389/fonc.2021.706733
9. Fan Y, Pan X, Yang F, et al. Preoperative computed tomography radiomics analysis for predicting receptors status and Ki-67 levels in breast cancer. *Am J Clin Oncol*. 2022;45(12):526–533. doi:10.1097/COC.0000000000000951
10. Ma W, Ji Y, Qi L, Guo X, Jian X, Liu P. Breast cancer Ki67 expression prediction by DCE-MRI radiomics features. *Clin Radiol*. 2018;73(10):909.e1–909.e5. doi:10.1016/j.crad.2018.05.027
11. Zhou J, Zhang Y, Chang KT, et al. Diagnosis of benign and malignant breast lesions on DCE-MRI by using radiomics and deep learning with consideration of peritumor tissue. *J Magn Reson Imaging*. 2020;51(3):798–809. doi:10.1002/jmri.26981
12. Li H, Zhu Y, Burnside ES, et al. MR imaging radiomics signatures for predicting the risk of breast cancer recurrence as given by research versions of MammaPrint, Oncotype DX, and PAM50 gene assays. *Radiology*. 2016;281(2):382–391. doi:10.1148/radiol.2016152110
13. Wang S, Wei Y, Li Z, Xu J, Zhou Y. Development and validation of an MRI radiomics-based signature to predict histological grade in patients with invasive breast cancer. *Breast Cancer*. 2022;14:335–342. doi:10.2147/BCTT.S380651
14. Takahashi H, Oshi M, Asaoka M, Yan L, Endo I, Takabe K. Molecular biological features of Nottingham histological grade 3 breast cancers. *Ann Surg Oncol*. 2020;27(11):4475–4485. doi:10.1245/s10434-020-08608-1
15. van Griethuysen J, Fedorov A, Parmar C, et al. Computational radiomics system to decode the radiographic phenotype. *Cancer Res*. 2017;77(21):e104–e107. doi:10.1158/0008-5472.CAN-17-0339
16. Wang S, Sun K, Wang L, et al. Breast tumor segmentation in DCE-MRI with tumor sensitive synthesis. *IEEE Trans Neural Netw Learn Syst*. 2021;34:4990–5001.
17. Mei F, Liu JY, Xue WC. 浸润性乳腺癌的组织学分级Nottingham组织学分级系统 [Histological grading of invasive breast carcinoma: Nottingham histological grading system]. *Zhonghua Bing Li Xue Za Zhi*. 2019;48(8):659–664. Chinese. doi:10.3760/cma.j.issn.0529-5807.2019.08.019
18. Zhu X, Ying J, Wang F, Wang J, Yang H. Estrogen receptor, progesterone receptor, and human epidermal growth factor receptor 2 status in invasive breast cancer: a 3198 cases study at national cancer center, China. *Breast Cancer Res Treat*. 2014;147(3):551–555. doi:10.1007/s10549-014-3136-y
19. Bahaddin MM. A comparative study between Ki67 positive versus Ki67 negative females with breast cancer: cross sectional study. *Ann Med Surg*. 2020;60:232–235. doi:10.1016/j.amsu.2020.10.049
20. Rakha EA, El-Sayed ME, Lee AH, et al. Prognostic significance of Nottingham histologic grade in invasive breast carcinoma. *J Clin Oncol*. 2008;26(19):3153–3158. doi:10.1200/JCO.2007.15.5986
21. Anderson TJ, Alexander FE, Lamb J, Smith A, Forrest AP. Pathology characteristics that optimize outcome prediction of a breast screening trial. *Br J Cancer*. 2000;83(4):487–492. doi:10.1054/bjoc.2000.1286
22. Heusinger K, Löhberg C, Lux MP, et al. Assessment of breast cancer tumor size depends on method, histopathology and tumor size itself*. *Breast Cancer Res Treat*. 2005;94(1):17–23. doi:10.1007/s10549-005-6653-x
23. Alduk AM, Brcic I, Podolski P, Prutki M. Correlation of MRI features and pathohistological prognostic factors in invasive ductal breast carcinoma. *Acta Clin Belg*. 2017;72(5):306–312. doi:10.1080/17843286.2016.1266432
24. Costantini M, Belli P, Rinaldi P, et al. Diffusion-weighted imaging in breast cancer: relationship between apparent diffusion coefficient and tumour aggressiveness. *Clin Radiol*. 2010;65(12):1005–1012. doi:10.1016/j.crad.2010.07.008

25. Kim KW, Kuzmiak CM, Kim YJ, Seo JY, Jung HK, Lee MS. Diagnostic usefulness of combination of diffusion-weighted imaging and T2WI, including apparent diffusion coefficient in breast lesions: assessment of histologic grade. *Acad Radiol*. 2018;25(5):643–652. doi:10.1016/j.acra.2017.11.011
26. Surov A, Clauser P, Chang YW, et al. Can diffusion-weighted imaging predict tumor grade and expression of Ki-67 in breast cancer? A multicenter analysis. *Breast Cancer Res*. 2018;20(1):58. doi:10.1186/s13058-018-0991-1
27. Liu X, Zhang J, Zhou J, et al. Multi-modality radiomics nomogram based on DCE-MRI and ultrasound images for benign and malignant breast lesion classification. *Front Oncol*. 2022;12:992509. doi:10.3389/fonc.2022.992509
28. He D, Wang X, Fu C, et al. MRI-based radiomics models to assess prostate cancer, extracapsular extension and positive surgical margins. *Cancer Imaging*. 2021;21(1):46. doi:10.1186/s40644-021-00414-6
29. Yu Y, Tan Y, Xie C, et al. Development and validation of a preoperative magnetic resonance imaging radiomics-based signature to predict axillary lymph node metastasis and disease-free survival in patients with early-stage breast cancer. *JAMA Netw Open*. 2020;3(12):e2028086. doi:10.1001/jamanetworkopen.2020.28086